Supplementary Information for:

Sticky-MARTINI as A Reactive Coarse-Grained Model for Molecular Dynamics Simulations of Silica Polymerization

André Carvalho[1], Sérgio M. Santos[1], Germán Pérez-Sánchez[1], Daniel Gouveia[1], José R. B. Gomes[1,], Miguel Jorge[2,*]*

[1]CICECO-Aveiro Institute of Materials, Department of Chemistry, University of Aveiro, Campus Universitário de Santiago, 3810-193 Aveiro, Portugal

[2]Department of Chemical and Process Engineering, University of Strathclyde, 75 Montrose Street, Glasgow G1 1XJ, United Kingdom

[*]Corresponding authors

José R. B. Gomes, University of Aveiro, Campus, Universitário de Santiago, Aveiro, Portugal; Phone: (+351) 234401423; E-mail address: jrgomes@ua.pt

Miguel Jorge, University of Strathclyde, 75 Montrose Street, Glasgow, United Kingdom Phone: (+44) 1415482825; E-mail address: miguel.jorge@strath.ac.uk

Supplementary Notes

Supplementary Note 1 - The acronyms used throughout the text are defined below.
AA – All-atom;
AA-MD – All-atom Molecular Dynamics;
CG – Coarse grained;
CTA^+ – Cetyltrimethylammonium cation;
LJ – Lennard-Jones;
MARTINI – General purpose coarse-grained force field;
MC – Monte Carlo;
MCM-41 – Mobil Composition of Matter # 41 (a periodic mesoporous silica material with hexagonal structure);
MD – Molecular Dynamics;
PMS – Periodic mesoporous silica;
P_{SN} – Coarse-grained bead for a neutral silicate monomer based on the MARTINI force field;
Q_{SI} – Coarse-grained bead for a singly negatively charged silicate monomer based on the MARTINI force field;
ReaxFF – A reactive force field;
RSi – Reactive silica bead (new topology from this work);
SP – Sticky particle;
SP_{SN} – Coarse-grained bead for a neutral silicate monomer based on the MARTINI 2.2 force field;
S_{Si} – Coarse-grained bead for a silicate monomer (generic) based on the MARTINI 2.2 force field;
SQ_{SI} – Coarse-grained bead for a singly negatively charged silicate monomer based on the MARTINI 2.2 force field;
TMA^+ – Tetramethylammonium cation;
VS – Virtual site.

Supplementary Note 2 - The symbols used throughout the text are defined below.
C_6 – Lennard-Jones attractive coefficient;
C_{12} – Lennard-Jones repulsive coefficient;
c – Degree of condensation;
d – Distance;
ε – Well-depth in the Lennard-Jones potential;
K_b – Bond force constant;
m – Mass;
q_i – Mole fraction with i being the number of coordinated neighbors (it can be 0, 1, 2, 3 and 4);
Q_n – Silicon coordination environment with n being the number of coordinated neighbors (it can be 0, 1, 2, 3 and 4);
σ – Distance at which the intermolecular Lennard-Jones potential between two particles is zero;
t – Time.

Supplementary Methods

A detailed list of composition and simulation times for the different systems studied in this work is provided in Supplementary Table 1.

Supplementary Table 1 – Parameters of an RSi particle, composed of a central S_{Si} MARTINI bead, four SP and four VS: masses (m), LJ parameters (σ and ε), intra-bead distances (d), and bond force constant (K_b).

	Neutral (Fig. 4)	Self-assembly (Fig. 5)	Encapsulation (Fig. 6 top)	Cationic (Fig. 6 bottom)
CTA^+	-	100	100	-
TMA^+	-	-	-	100
SI	-	100	100	100
SN	1000	-	200	200
Water	6500	56250	56250	56250
Anti-freeze	1200	6250	6250	6250
Time (μs)	8.4	3.2	4.6	3.0
pH (estimated)	2.5	>12	9.5	9.5

In order to develop a more realistic reactive CG silica model to represent the distance between adjacent groups in silica oligomers, we replaced the original Q_{SI} interaction bead with a smaller SQ_{SI} bead. This changes only the self-interactions of this bead, while interactions between silica and all the other molecules in the system remain the same. We would expect this to have a minimal effect on the properties of the system. To confirm this, we carried out simulations on a pre-formed micelle with 100 CTA^+ surfactants and 100 anionic silicic acid monomers, using both our original Q_{SI} model and the modified SQ_{SI} model. As can be seen in the Supplementary Figure 1, the two sets of profiles are practically indistinguishable, confirming that the behaviour of the anionic silicates, in terms of interactions with the surfactant micelles, is unchanged by this modification.

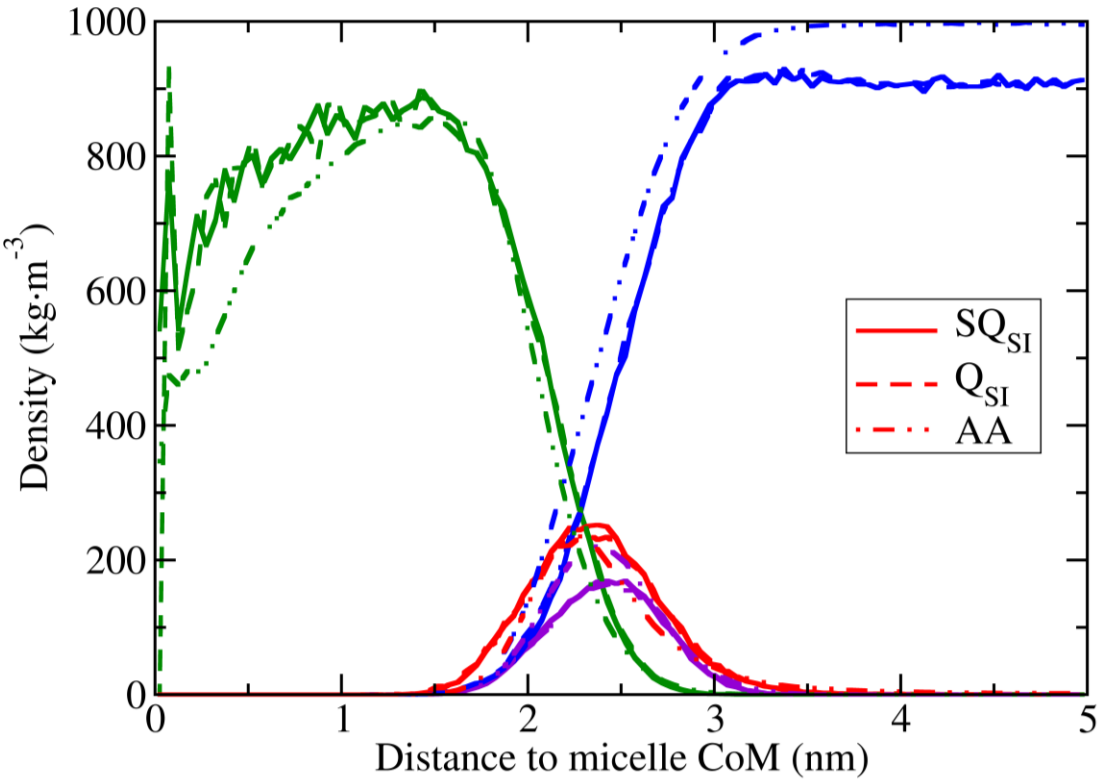

Supplementary Figure 1 – Density profiles for a pre-formed micelle with 100 CTA^+ surfactants and 100 anionic silica monomers. Surfactant tails are shown in green, surfactant heads in purple, silica in red, and water in blue. The solid lines correspond to the original Q_{SI} model, the dashed lines correspond to the modified SQ_{SI} model, and the thin dashed-dotted lines correspond to the reference atomistic model.

Supplementary Discussion

The accuracy of the simulated silica condensation process is limited by an extremely sensitive balance between the repulsion forces of the VS and the attractive LJ potential between intermolecular SP. When both, ε_{SP} and ε_{rep}, are fixed to 0 kJ mol^{-1}, the interactions involving the SP and VS are turned off and the model resembles the one proposed by Pérez-Sánchez *et al.*[1]. This configuration displays a spherical energy profile due to the lack of these intermolecular interactions, and although transient contacts between silica particles do occur during the simulation, no bonding as such is observed. When the ε_{SP} and ε_{rep} parameters are both finite, the reactive silica model is activated and formation of condensed systems is promoted, controlled by the delicate balance between these two parameters. On the one hand, the attractive SP-SP interactions need to be strong enough to promote binding that is sufficiently long-lived, as in the realistic case of a chemical reaction. In fact, when the $\varepsilon_{SP}/\varepsilon_{rep}$ ratio was too low, only poorly condensed systems were formed (Supplementary Figure 2d). This was caused by the attractive SP-SP force not being strong enough to counter the remaining forces in the system. In this case, one observes a quick formation and breakage of connections, with more condensed species becoming less favourable.

On the other hand, the range and directionality of the attractive interaction (controlled by the interplay with the VS-SP repulsion) should not allow for coordination to more than 4 neighbours, thus respecting the tetrahedral structure of silica networks. In the limit where the range of the SP-SP interaction is very large, each SP can bind more than one silica monomer (labelled as Q_{5+} in the condensation progress plots) and possibly even lead to an *fcc* packing of the silica particles. Indeed, for some combinations of parameters, we observed the formation of rather stable "triple bonds", as illustrated in Supplementary Figure 2a, equivalent to an oxygen atom unrealistically bridging three silica atoms. During a simulation, the vibration of a perfectly condensed silica core can lead to the formation of these triple bonds in the bulk. Due to their apparent stability at very large $\varepsilon_{SP}/\varepsilon_{rep}$ ratios, the occurrence of these configurations was highly probable and usually irreversible. Therefore, if ε_{rep} is unable to shield the attraction due to ε_{SP}, a higher rate of condensation is obtained, resulting in unrealistically low mole fractions of Q_1 and Q_2 species and non-negligible fractions of Q_{5+} species (Supplementary Figure 2b, yellow line). Our choice of values for the ε_{rep} and ε_{SP} parameters ensured that the correct experimental condensation profile

was reproduced, while maintaining unrealistic Q_{5+} species to a minimum (Supplementary Figure 2c; please see main paper for a detailed comparison with experimental data).

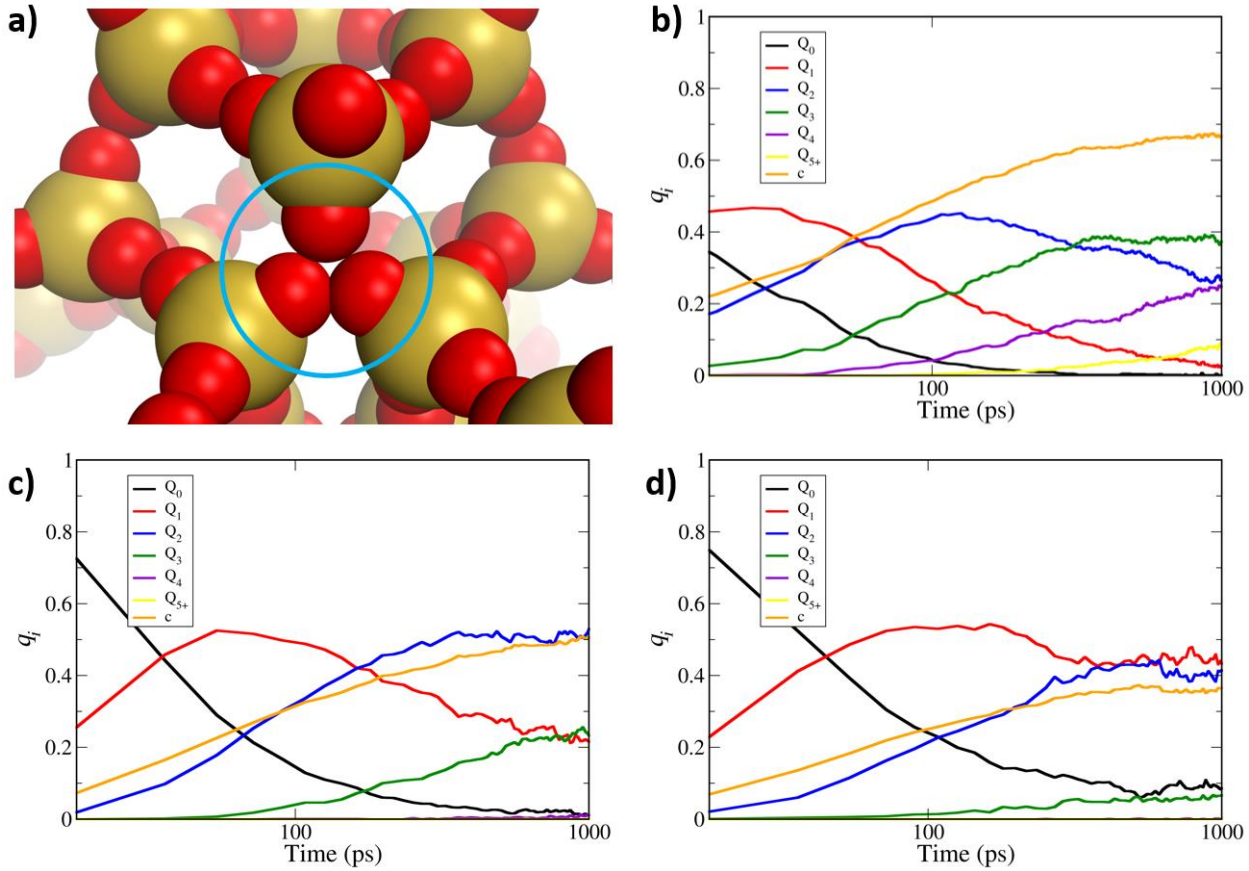

Supplementary Figure 2 – a) Representation of a triple bond between reactive silica monomers, highlighted by the blue circle. Red and gold spheres represent sticky particles (SP) and SQ_{SI} particles, respectively. For ease of visualization, water beads and virtual sites are not shown. Evolution of the molar fractions (q_i) of the silicon coordination environment (Q_n) calculated for ε_{SP} = 50 kJ/mol and b) $\varepsilon_{rep} = 0.10 \times 10^{-5}$ kJ/mol; c) $\varepsilon_{rep} = 0.24 \times 10^{-5}$ kJ/mol and d) $\varepsilon_{rep} = 0.30 \times 10^{-5}$ kJ/mol.

In the case of the neutral system, we track in Supplementary Figure 3 the dynamic evolution of a pair of silicate monomers (highlighted in full colour) during a stage of the simulation in which they approach each other in solution, form a "covalent bond", and then this bond breaks due to particle collisions. This process of bond formation and breakage was observed frequently during simulations with our reactive CG silica model.

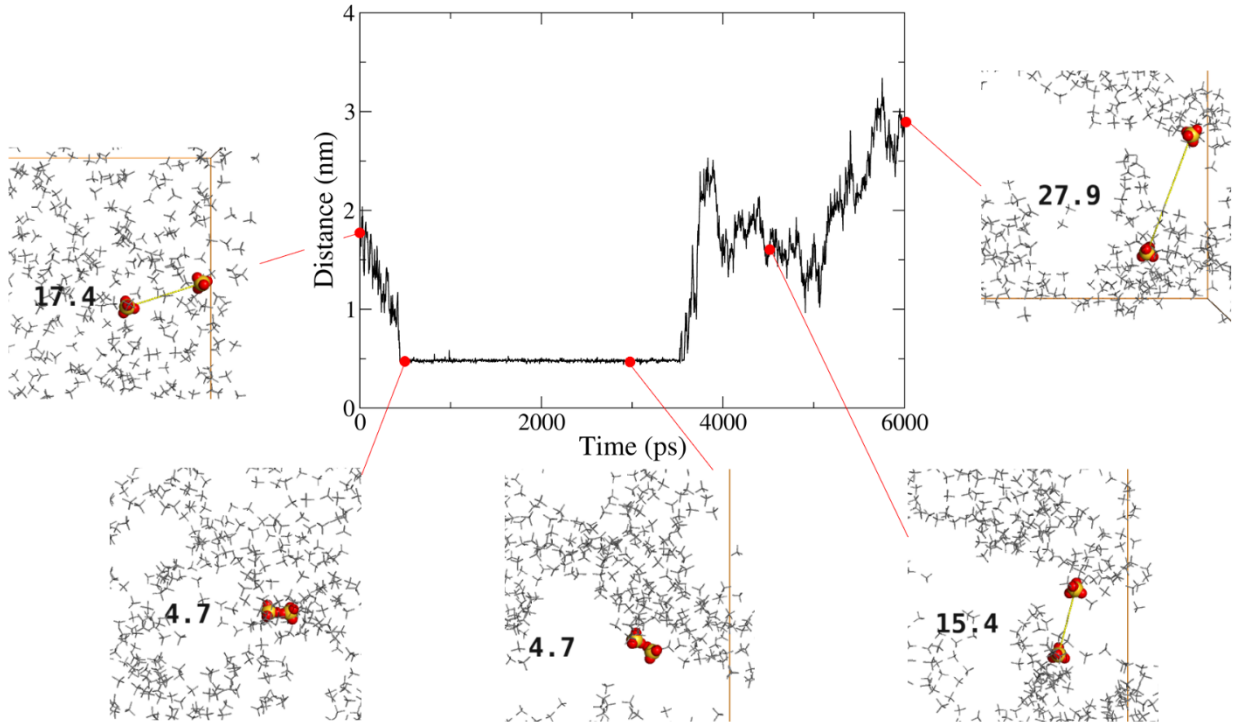

Supplementary Figure 3 – Profile tracking the distance between two silica monomers as they approach each other, bond to form a dimer, and then dissociate. The insets show close-up snapshots at times indicated by the red dots on the profile. The two monomers that were tracked are shown in full colour (colour code as in Supplementary Figure 2), while other silicates are shown as grey sticks. The labels in each snapshot indicate the distance between the two monomers in Å.

In Supplementary Figure 4, we show the distributions of Si-Si distances (defined here as the distance between two SQ_{SI} particles in adjacent silicates) as well as of Si-O-Si angles (defined here as the angle between two SQ_{SI}-SP vectors in adjacent silicates). As we can see, the distance distribution is quite narrow, centred around ~0.482 nm, while the angle distribution is broader, with an average of ~152º.

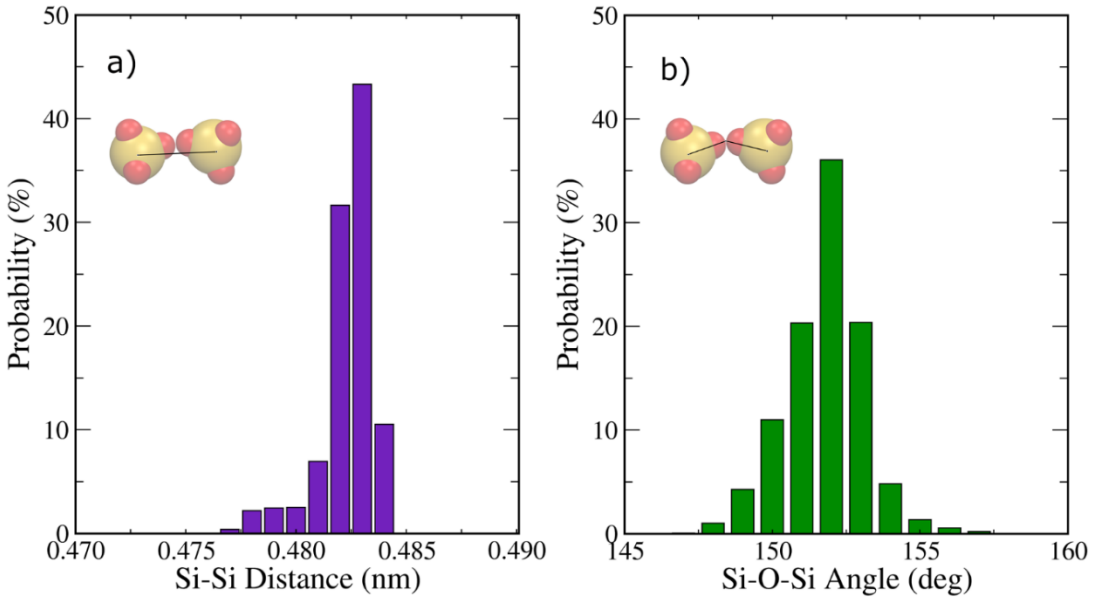

Supplementary Figure 4 – Distributions of SQ_{SI}-SQ_{SI} distances (a) and SQ_{SI}-SP|SP-SQ_{SI} angles (b) of the bonded silica species obtained from reactive MD simulations of a neutral silica solution. The insets show diagrams depicting how the bond and angle, respectively, were defined.

In Supplementary Figure 5, we show the time evolution of the total number of clusters, as well as the average and maximum cluster size, during the MD simulation of the neutral silica solution undergoing polymerization reactions using our new CG reactive silica model.

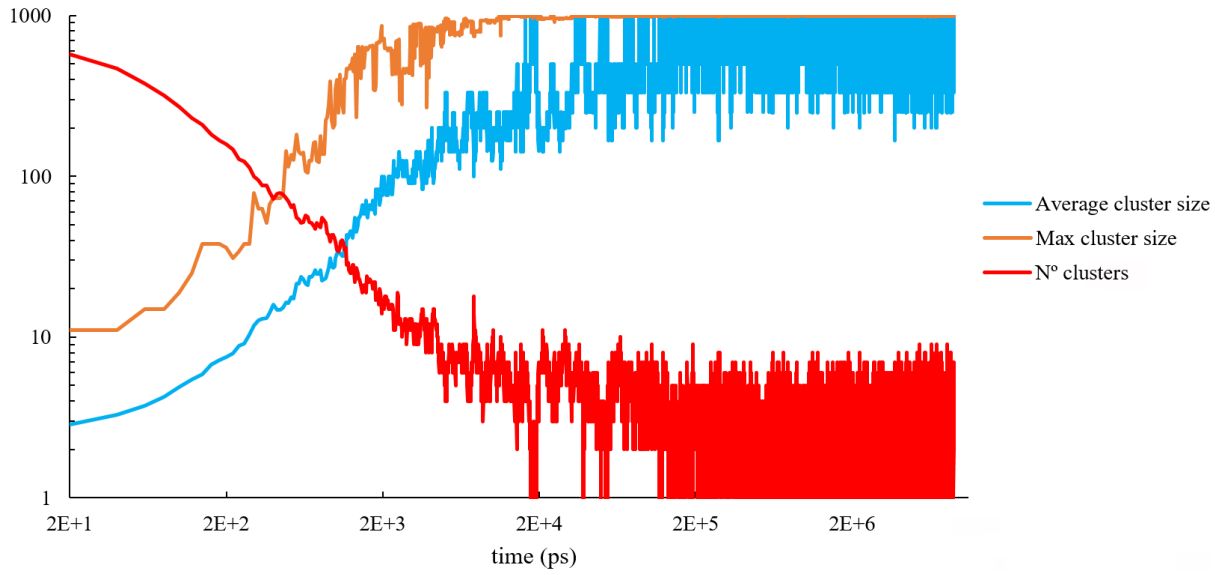

Supplementary Figure 5 – Average and maximum cluster sizes as well as total number of clusters observed during the MD simulation of the neutral silica polymerization system.

At the simulations times for which the maximum of q_1 (54 ps) species was reached, the system is composed by mostly linear chains with 3 to 5 monomers. Eventually, these small chains come together and can form longer chains as can be seen in Supplementary Figure 6a. Branched silicates are also seen (cf. main paper). After the maximum of q_1 (54 ps) species is reached, all these structures start to cyclize to form ring structures, with one of those structures obtained at 380 ps (q_2 peak maximum) depicted in Supplementary Figure 6b.

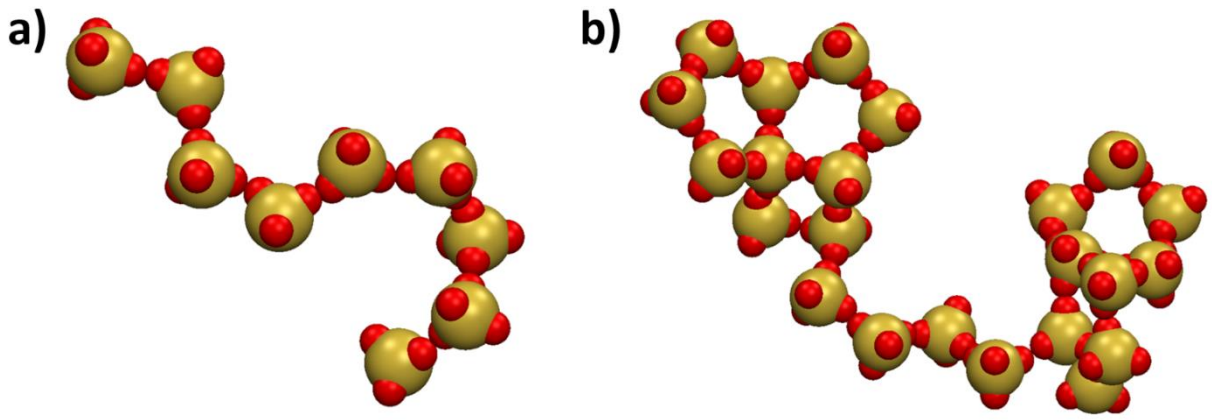

Supplementary Figure 6 – Linear nonamer (a) and two cyclic structures linked by a linear tetramer (b) observed during the MD simulation of the neutral silica polymerization system. Colour codes as in Supplementary Figure 2.

As discussed in the main paper, the time scales for the MD simulations and experimental measurements differed by several orders of magnitude. In Supplementary Figure 7, we attempt to apply a simple scaling factor (the chosen value was 2×10^{13}) to the simulation data (solid lines) so that it can be mapped onto and directly compared to the experimental profiles (dashed lines and symbols). As can be seen, the agreement is very reasonable but it appears that successive "key events" of the condensation profile (e.g. peak positions in individual q_i curves and intersections between different q_i curves) seem to take place relatively earlier in the simulations than in the experiments.

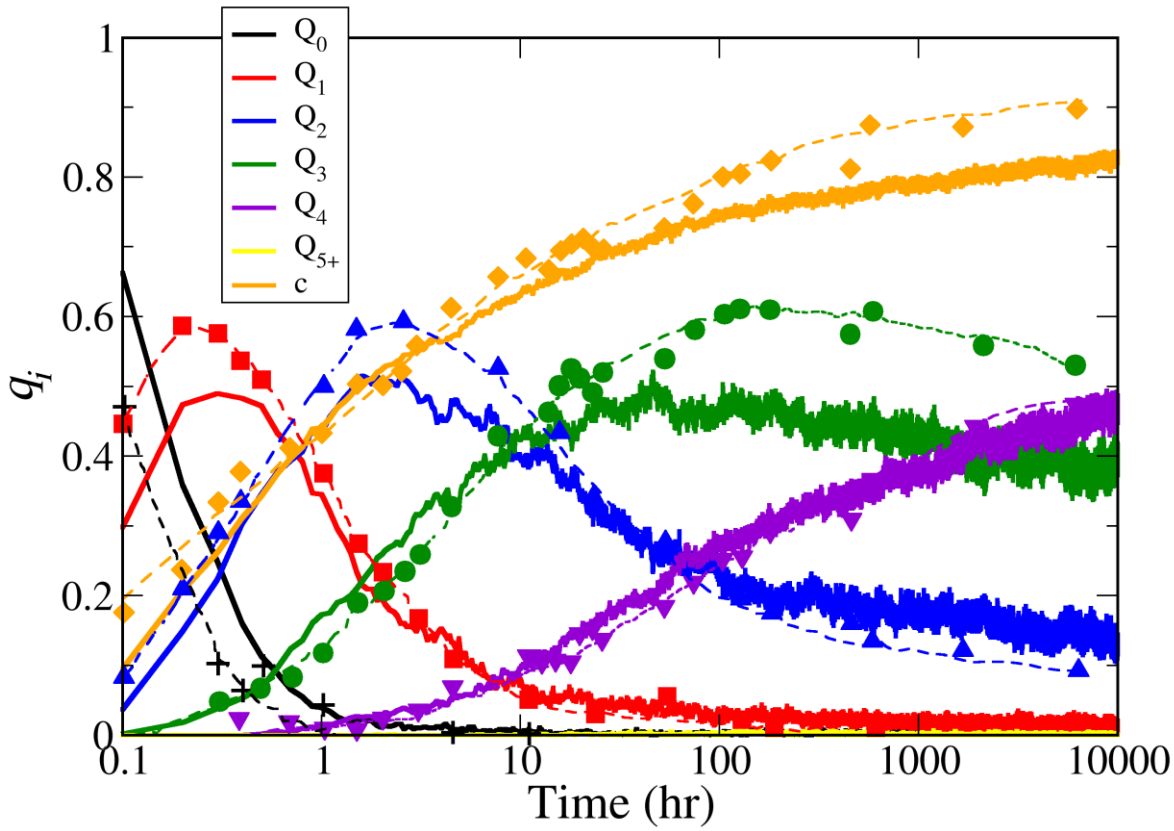

Supplementary Figure 7 – Comparison between the experimental time evolution of profiles for the molar fraction (q_i) of the silicon coordination environment (Q_n), represented by symbols and thin dashed lines, and the MD simulation profiles after application of a scaling factor of 2×10^{13}, represented by solid lines.

This can be ascertained in more detail in Supplementary Figure 8, where we show a plot of the "optimal" scaling parameter that matches each successive intersection point between different q_i curves. From this analysis, it is possible to discern three stages of acceleration of the reaction, each of them corresponding to the onset of a maximum mole fraction in each Q_n profile. The first stage corresponded to the first 60 ps of simulation, when the system yielded dimers, with the simulated reaction ~1.2×10^{13} times faster than the experiment. The transition to the next stage occurred approximately at the maximum mole fraction of Q_1. In the second stage, the reaction rate was ~1.6×10^{13} faster than experiments. Here, the fast nucleation of silica dimers and monomers produced Q_2 species. As soon as the maximum mole fraction of these species was achieved, the system progressed to the next stage, with the reaction rate varying between ~2.2×10^{13} and ~2.9×10^{13} times faster than experiments. In this stage, the fast aggregation of dimers and trimers

promoted the formation of large amorphous structures of silica. In the remaining simulation time, these structures grew, with bond breaking and further rearrangement between structures. Extrapolating the results from Devreux *et al.*[2], one finds that the Q_3/Q_4 crossing would occur at ~ 9000 hours, meaning that the last phase of the condensation reaction has been accelerated ~10^{14} times relatively to the experimental reaction time.

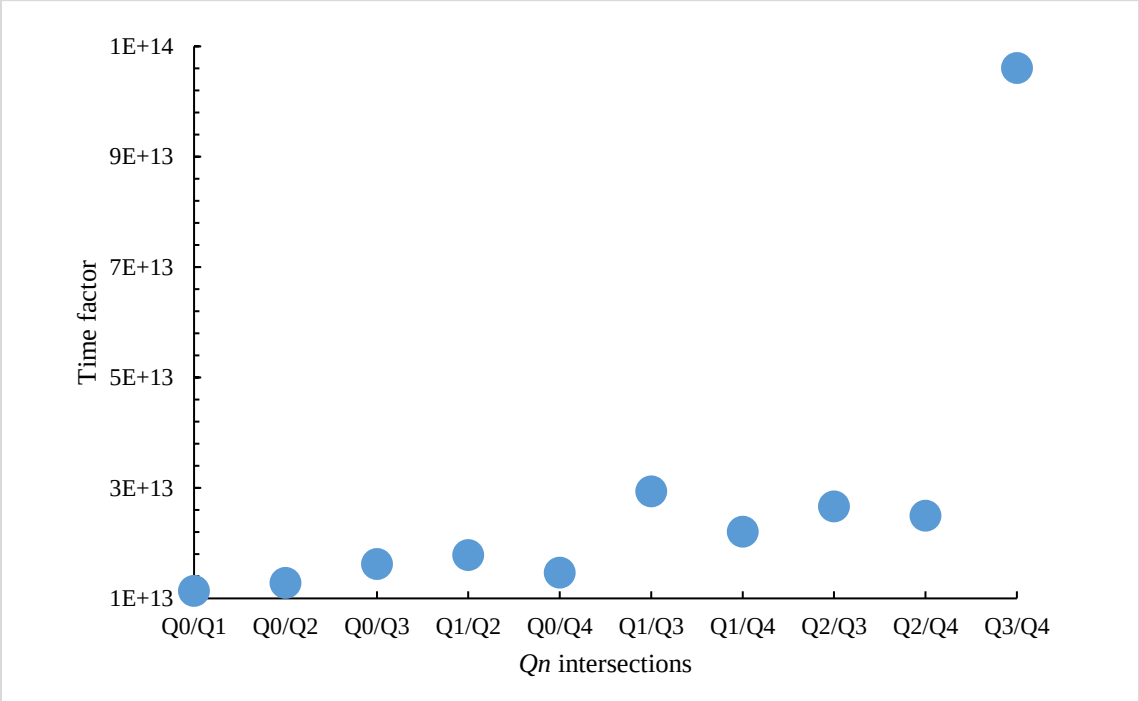

Supplementary Figure 8 – Ratio between experimental and simulation times at each Q_n intersection, sorted in chronological order.

In the case of the charged systems, snapshots from a micelle encapsulation simulation that started from a disordered distribution of molecules are shown in Supplementary Figure 9. The system tends towards the same equilibrium state as the simulation discussed in the main paper – i.e. a single micelle encapsulated by silica. While a single micelle is found for simulation times above ~0.70 μs, the structure of the silica shell surrounding the micelle is continuously evolving towards a more condensed structure, as can be clearly understood from the comparison of the molar fractions of Q_3 and Q_4 species and of Q_0, Q_1 and Q_2 shown in Supplementary Figure 10.

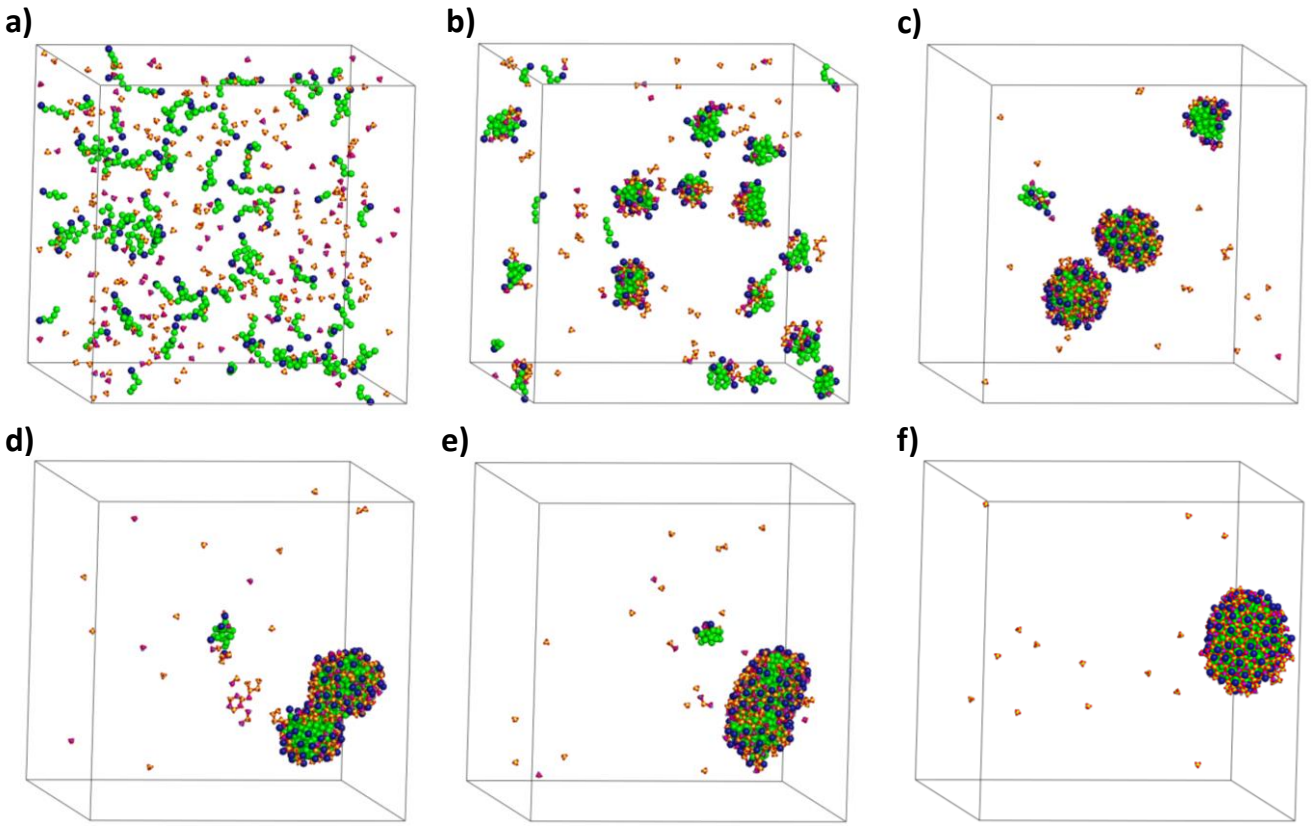

Supplementary Figure 9 – Snapshots of the micelle self-assembly simulation with polymerization reactions starting from a random distribution: a) Starting random distribution (t = 0.00 μs); b) Initial formation of small proto-micelles surrounded by silica monomers and small oligomers (t = 0.02 μs); c) Co-existence of small proto-micelles surrounded by small silica oligomers with small micelles surrounded by incomplete silica shells (t = 0.36 μs); d, e) Fusion of two micelles into a larger micelle (t = 0.50 μs); f) Snapshot with a single surfactant micelle surrounded by a layer of silica (t = 1.75 μs). Surfactant tails are shown in green, surfactant heads in dark blue, the central anionic/neutral silica beads are shown in purple/gold, and reactive/inactive SP are shown in red/grey. Water and VS were removed for ease of visualization.

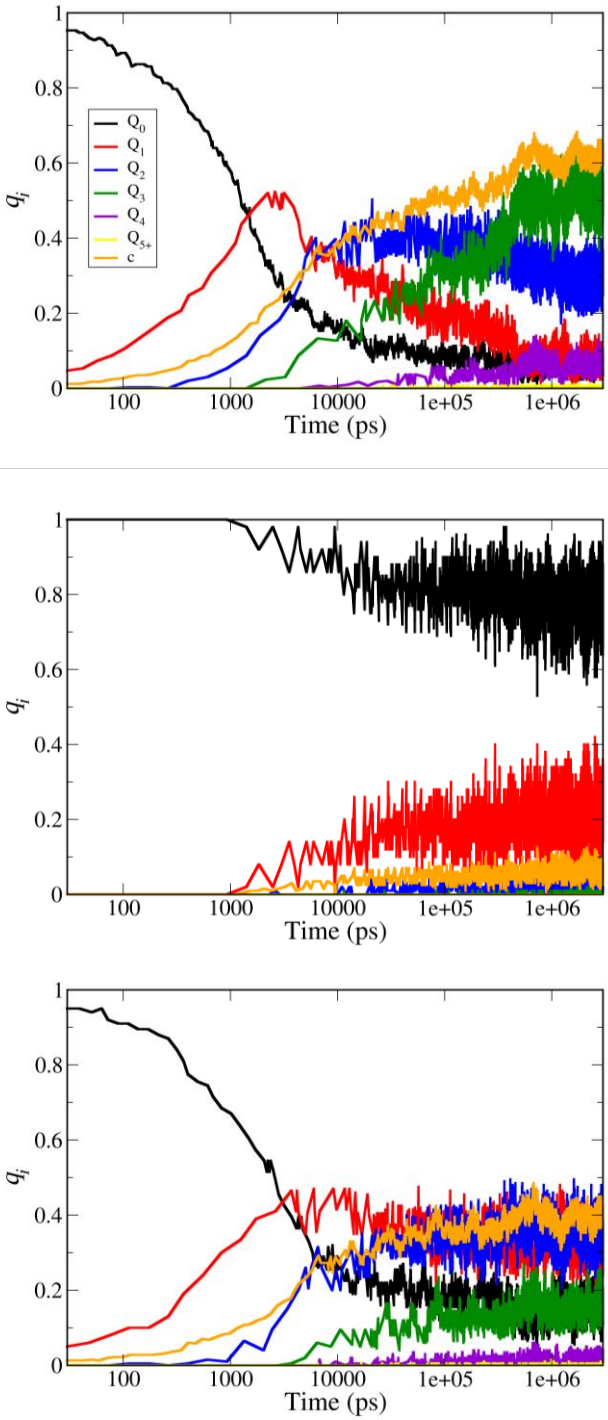

Supplementary Figure 10 – Time dependence of the molar fraction of each Q_n species during the reactive MD simulations of the micelle encapsulation where both self-assembly and reaction proceeded simultaneously from the beginning of the simulation. Top, middle and bottom panels show data for reactions between all RSi particles in the system, for reactions between anionic RSi^- particles only, and for reactions between neutral RSi_n particles only, respectively.

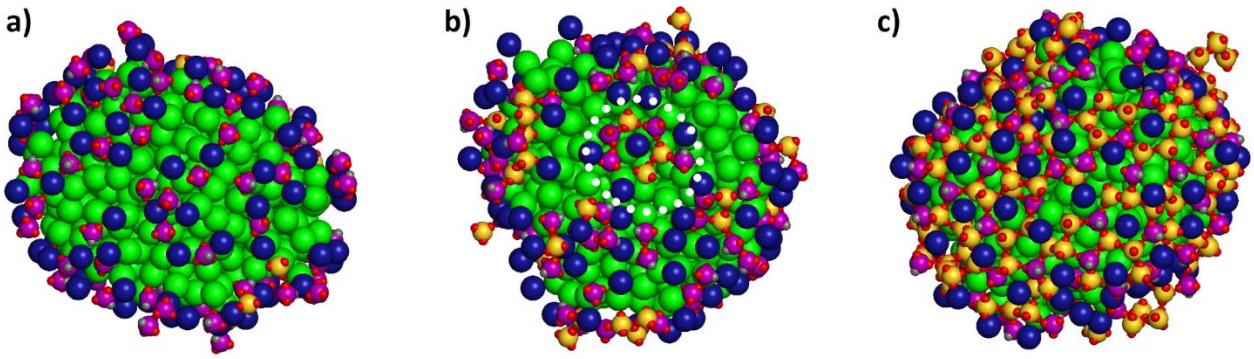

Supplementary Figure 11 – Closer views of the micelles formed during the micelle encapsulation simulation: a) Micelle formed without activation of the reactivity showing mostly RSi^- adsorbed at the surface (Figure 6b); b) and c) Micelles formed with activation of the reactivity, taken from Figures 6c and 6d, respectively, showing increasing degrees of oligomerization not only happening with RSi^- units already adsorbed at the surface but also with RSi_n adsorbed from solution, with one good example indicated with a white dotted circle in panel b). Colour code as in Supplementary Figure 9. Water and VS were removed for ease of visualization

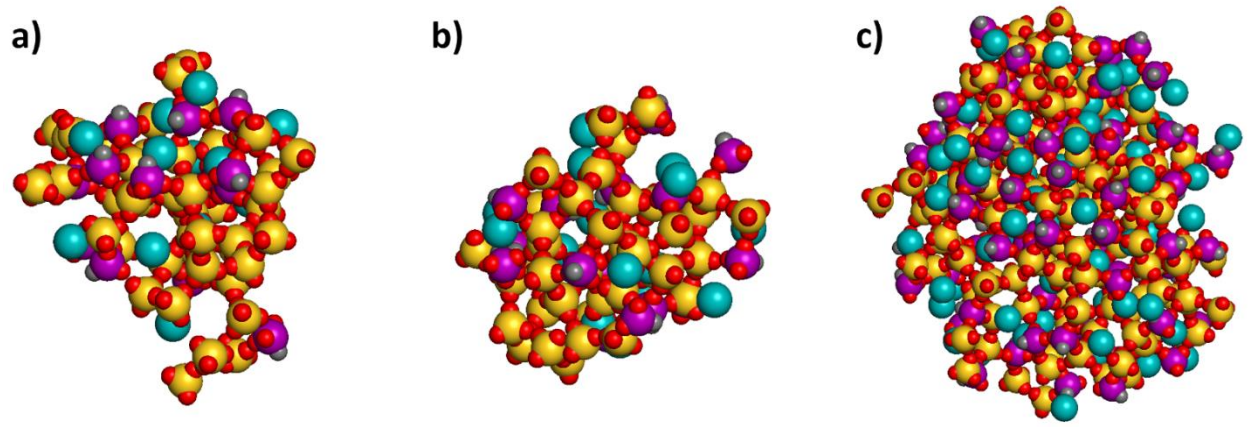

Supplementary Figure 12 – Closer views of the aggregates formed during the simulation with TMA^+ cations: a) and b) Small clusters from the simulation box shown in Figure 6f. c) Large amorphous silica structure incorporating several cations from the simulation box shown in Figure 6h. The central anionic/neutral silica beads are shown in purple/gold, reactive/inactive SP are shown in red/grey and TMA^+ beads are cyan. Water and VS were removed for ease of visualization.

Supplementary Figures 11 and 12 show detailed views of structures found in the simulations of the micelle encapsulation with silica (neutral and anionic species) and with TMA^+ cations, respectively. Snapshots of the final large aggregate shown in Supplementary Figure 12c are shown in Supplementary Figure 13, with layers of silicates and cations progressively removed, to allow a better understanding of the amorphous nature of the structure obtained and the incorporation of TMA^+ cations, both at the surface and below the external surface of the particle.

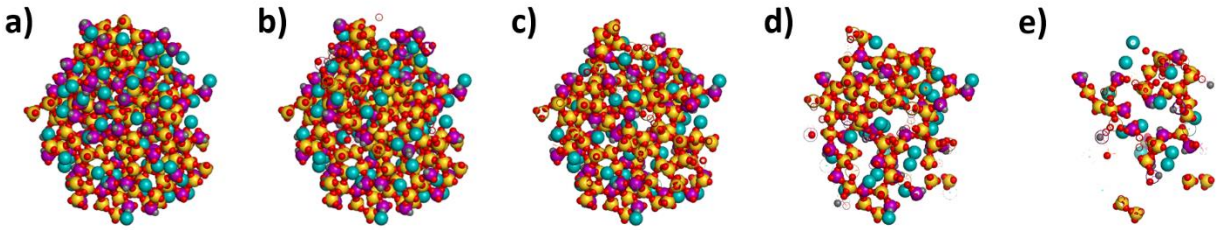

Supplementary Figure 13 – Snapshots of the large aggregate formed during the simulation with TMA^+ cations where from a) to e) silicates and TMA^+ cations closer to the viewer were progressively removed. Colour code as in Supplementary Figure 10. Water and VS were removed for ease of visualization.

Supplementary Figure 14 shows snapshots of the encapsulated micelle formed in the micelle encapsulation simulation shown in the top panels of Figure 6. Surfactants and silicates were progressively removed to allow a better understanding of the hollow silica capsule.

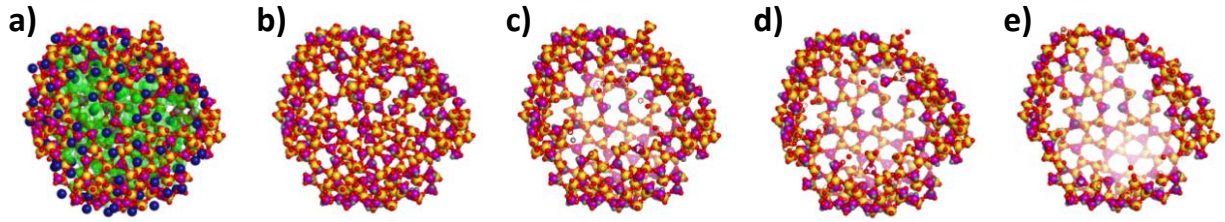

Supplementary Figure 14 – Snapshots of the micelle formed in the micelle encapsulation simulation. a) View of the surfactant micelle covered with the silica shell; b) hollow silica shell (i.e., surfactants were removed); and c) - e) silica shell where silicates closer to the viewer were progressively removed. Colour code as in Supplementary Figure 7 and with neutral silica beads shown in yellow. Water and VS were removed for ease of visualization.

Supplementary References

1. Pérez-Sánchez, G., Gomes, J. R. B. & Jorge, M. Modeling Self-Assembly of Silica/Surfactant Mesostructures in the Templated Synthesis of Nanoporous Solids. *Langmuir* **29**, 2387–2396 (2013).

2. Devreux, F., Boilot, J. P., Chaput, F. & Lecomte, A. Sol-gel condensation of rapidly hydrolyzed silicon alkoxides: A joint ^{29}Si NMR and small-angle x-ray scattering study. *Phys. Rev. A* **41**, 6901–6909 (1990).